**Atmospheric
Chemistry
and Physics**

Yields of oxidized volatile organic compounds during the OH radical initiated oxidation of isoprene, methyl vinyl ketone, and methacrolein under high-NO$_x$ conditions

M. M. Galloway[1,*], A. J. Huisman[1,**], L. D. Yee[2], A. W. H. Chan[3,***], C. L. Loza[3], J. H. Seinfeld[2,3], and F. N. Keutsch[1]

[1]Department of Chemistry, University of Wisconsin-Madison, Madison, WI, USA
[2]Division of Engineering and Applied Science, California Institute of Technology, Pasadena, CA, USA
[3]Division of Chemistry and Chemical Engineering, California Institute of Technology, Pasadena, CA, USA
*now at: Department of Chemistry, Reed College, Portland, OR, USA
**now at: Institute for Atmosphere and Climate, ETH Zurich, Zurich, Switzerland
***now at: Department of Environmental Science, Policy and Management, University of California, Berkeley, CA, USA

Abstract. We present first-generation and total production yields of glyoxal, methylglyoxal, glycolaldehyde, and hydroxyacetone from the oxidation of isoprene, methyl vinyl ketone (MVK), and methacrolein (MACR) with OH under high NO$_x$ conditions. Several of these first-generation yields are not included in commonly used chemical mechanisms, such as the Leeds Master Chemical Mechanism (MCM) v. 3.2. The first-generation yield of glyoxal from isoprene was determined to be 2.1 ($\pm$0.6) %. Inclusion of first-generation production of glyoxal, glycolaldehyde and hydroxyacetone from isoprene greatly improves performance of an MCM based model during the initial part of the experiments. In order to further improve performance of the MCM based model, higher generation glyoxal production was reduced by lowering the first-generation yield of glyoxal from C5 hydroxycarbonyls. The results suggest that glyoxal production from reaction of OH with isoprene under high NO$_x$ conditions can be approximated by inclusion of a first-generation production term together with secondary production only via glycolaldehyde. Analogously, methylglyoxal production can be approximated by a first-generation production term from isoprene, and secondary production via MVK, MACR and hydroxyacetone. The first-generation yields reported here correspond to less than 5 % of the total oxidized yield from isoprene and thus only have a small effect on the fate of isoprene. However, due to the abundance of isoprene, the combination of first-generation yields and reduced higher generation production of glyoxal from C5 hydroxycarbonyls is important for models that include the production of the small organic molecules from isoprene.

1 Introduction

Isoprene (2-methyl-1,3-butadiene) is emitted into the atmosphere from vegetation in large quantities ($\sim$500 Tg year^{-1}) (Guenther et al., 1995). Globally, the dominant atmospheric sink of isoprene is reaction with the OH radical (Archibald et al., 2010a). Due to its reactivity with the OH radical and high mixing ratios in forested areas, isoprene has important impacts on the oxidative capacity of the atmosphere (Karl et al., 2009). OH oxidation of isoprene has been studied in detail, and there are a number of commonly used explicit chemistry mechanisms such as the Leeds Master Chemical Mechanism (MCM), Mainz Isoprene Mechanism (MIM) or the NCAR Master Mechanism (Madronich and Calvert, 1989; Jenkin et al., 1997; Saunders et al., 2003; Taraborrelli et al., 2009). Oxidation of isoprene initiated by OH is an important source of small carbonyls and hydroxycarbonyls, such as glyoxal, methylglyoxal, and glycolaldehyde. These species are of interest within the context of cloud processing and secondary organic aerosol (SOA) formation (Carlton et al., 2007; Altieri et al., 2008; Ervens et al., 2008; Galloway et al., 2009; Ip et al., 2009; Nozière et al., 2009; Perri et al., 2009; Shapiro et al., 2009; Tan et al., 2009; Volkamer et al., 2009; Sareen et al., 2010; Galloway et al., 2011). To quantify the atmospheric impacts of these compounds, it is important

Table 1. First-generation yields from high NO$_x$ experiments. All yields and errors are in percent. All uncertainties presented in this work represent the 1σ error. The MCM yields are calculated for the reaction with OH and on the basis that the fate of peroxy radicals is dominated by NO with negligible contribution from reaction with HO$_2$ or RO$_2$.

Compound	MVK	MACR	Glycolaldehyde	Hydroxyacetone	Glyoxal	Methylglyoxal
Isoprene[a]	$30.4\pm1.3\%$	$22.01\pm0.62\%$	$2.69\pm0.82\%$	$2.9\pm0.051\%$	$2.10\pm1.2\%$	ND
Isoprene[b]	$29\pm7\%$	$21\pm5\%$				
Isopren e[c]	40%	26%	4.2%	3.8%	**3.8%	**4.2%
Isoprene[g]	41.5%	26.5%	NI	NI	NI	NI
Isoprene[h]	NI	NI	NI	NI	0.3–3.0%	NI
MVK[a]			$67.4\pm3.0\%$	*0%	*0%	$24.12\pm0.14\%$
MVK[d]			$64\pm8\%$			$25\pm4\%$
MVK[c]			62.5%			**26.5%
MVK[g]			70%	NI	NI	29%
MACR[a]			*0%	$39.5\pm1.7\%$	*0%	$8.09\pm0.45\%$
MACR[e]				$41\pm3\%$		$8.4\pm1.6\%$
MACR[f]				$47\pm5\%$		<12%
MACR[c]				20%		**0%
MACR[g]			NI	43%	NI	NI

ND = no data. NI = not included in the MCM. [a] This work [b] Tuazon and Atkinson (1990a). [c] Paulot et al. (2009a). [d] Tuazon and Atkinson (1989). [e] Tuazon and Atkinson (1990b). [f] Orlando et al. (1999). [g] MCM [h] Volkamer et al. (2006). * 0% within uncertainty of measurement. ** Inferred from the presented mechanism from that study.

to understand their tropospheric production via oxidation of volatile organic compounds (VOCs), isoprene in particular.

Atmospheric isoprene oxidation has long been of interest (Gu et al., 1985; Tuazon and Atkinson, 1990a; Paulson et al., 1992; Miyoshi et al., 1994; Kwok et al., 1995; Sprengnether et al., 2002; Fan and Zhang, 2004; Zhao et al., 2004; Carlton et al., 2009; Karl et al., 2009; Paulot et al., 2009a; Archibald et al., 2010a,b). Tuazon and Atkinson (1990a) studied isoprene oxidation in the presence of OH and NO$_x$, and determined first-generation formation yields of methyl vinyl ketone (MVK), methacrolein (MACR), and formaldehyde (see Table 1 for all yields). The same authors also determined first-generation photooxidation yields of glycolaldehyde and methylglyoxal from MVK as well as yields of hydroxyacetone, methylglyoxal, and CO from MACR (Tuazon and Atkinson, 1989, 1990b). Orlando et al. (1999) studied OH-initiated MACR oxidation in the presence of NO$_x$ and quantified hydroxyacetone as a product. Based on their detection limit for methylglyoxal, they were able to infer an upper limit of 12% for the first-generation methylglyoxal yield from MACR.

While all of these studies have added to our mechanistic understanding of isoprene oxidation, recent measurements point to gaps in our understanding of isoprene oxidation (Dibble, 2004a,b; Volkamer et al., 2006; Paulot et al., 2009a). The existing master mechanisms cited above specify glyoxal as a higher generation oxidation product of isoprene, but few studies exist in which glyoxal, methylglyoxal, glycolaldehyde, or hydroxyacetone are measured in isoprene oxidation. One such study compared first-generation MACR and glyoxal to derive a first-generation glyoxal yield of 0.3–

3% (Volkamer et al., 2006). Theoretical work by Dibble (2004a,b) suggests a mechanism for such first-generation glyoxal and methylglyoxal formation from isoprene under high NO$_x$ conditions, specifically that glyoxal, methylglyoxal, glycolaldehyde, and hydroxyacetone can be formed through rapid isomerisation and double intramolecular hydrogen transfer of alkoxy radical intermediates. Glycolaldehyde and methylglyoxal are produced together in the suggested mechanism, as are glyoxal and hydroxyacetone. Paulot et al. (2009a) also studied isoprene oxidation, focusing on the isoprene δ-hydroxy oxidation channel. They observed first-generation yields of glycolaldehyde and hydroxyacetone and inferred the same yields for methylglyoxal and glyoxal, respectively, based on the work of Dibble (2004a,b) as they had no measurements of the dicarbonyls.

The work presented here studies the formation of a number of first- and higher-generation products formed during OH oxidation of isoprene, MVK, and MACR under high NO$_x$ conditions. First-generation yields from these precursors are incorporated into a zero-dimensional photochemical box model (Huisman et al., 2011) based on the MCM v. 3.2 (Jenkin et al., 1997; Saunders et al., 2003) to evaluate the extent to which the model can represent experimental measurements.

2 Experimental procedures

Experiments were carried out in the Caltech dual 28 m^3 Teflon chambers, described in detail elsewhere (Cocker et al., 2001; Keywood et al., 2004). See Tables 2 and S1 for experimental conditions. Temperature, relative humidity (RH),

Table 2. Experiment list.

Exp. #	Date (mm/dd/yy)	Compound	Initial conc. (ppb)	Initial NO (ppb)	Initial NO$_2$ (ppb)	RH (%)	T (K)	Lights	OH source
Chan 1*	02/06/08	Glyoxal	499	3	3	3	298	50 %	None
1	07/21/10	Glyoxal	64	3	21	4	294	50 %	None
2	02/02/08	Isoprene	603	466	606	4	293	10 %	HONO
3	02/04/08	Isoprene	609	465	550	5	294	10 %	HONO
4	10/15/09	Isoprene	187	361	675	8	295	10 %	HONO
5	10/17/09	Isoprene	17	250	403	9	295	10 %	HONO
6	10/19/09	Isoprene	187	307	545	10	294	10 %	HONO
7	07/22/10	Isoprene	60	325	527	4	293	10 %	HONO
8	10/21/09	MVK	25	279	534	10	295	10 %	HONO
9	07/20/10	MVK	20	294	523	4	294	10 %	HONO
10	10/23/09	MACR	42	231	437	7	295	10 %	HONO
11	10/25/09	Blank	None	250	455	8	294	10 %	HONO

* Chan et al. (2009).

O$_3$, NO, and NO$_x$ were continuously monitored. RH was held at ∼10 % throughout the experiments to prevent losses to chamber walls, although the reactions studied here are not sensitive to RH. Therefore the yields determined in this work should be applicable to higher RH. The wavelength of the chamber black lights is centered at 350 nm, and at 50 % power, the lights have a spectral intensity equivalent to $J_{NO_2} = 0.2366\,\text{min}^{-1}$.

Gas-phase isoprene, MVK, and MACR were monitored by gas chromatography with a flame ionization detector (GC-FID, Agilent 6890N). Gas-phase glyoxal was continuously monitored using the Madison laser induced phosphorescence instrument described by Huisman et al. (2008). This instrument was operated at 30 s time resolution, with a limit of detection (3σ) for glyoxal of 2.9 ppt in 30 s. Calibrations are performed with the same methods described for glyoxal by Huisman et al. (2008). Methylglyoxal was also measured with this instrument by subtracting glyoxal and background signals from the total α-dicarbonyl signal to give the methylglyoxal signal and Exps. 7 and 9 (Table 2) also utilized the lifetime methylglyoxal detection method described by Henry et al. (2011). Briefly, this method monitors the phosphorescence decay of glyoxal and methylglyoxal after each laser pulse and uses the known lifetimes of those decays to determine the contribution of each compound to the total signal. More details can be found in the supplemental information.

A chemical ionization mass spectrometer (CIMS) was used for online gas-phase measurement of glycolaldehyde and hydroxyacetone. The CIMS consists of a custom chemical ionization source connected to a Varian 1200 triple quadrupole mass spectrometer, previously described in detail (Crounse et al., 2006; Paulot et al., 2009b; St. Clair et al., 2010). Negative-mode operation utilized CF$_3$O$^-$ ions that cluster with the analyte detected at *m/z* MW + 85 or via fluoride transfer for more acidic species detected at

m/z MW + 19. Positive-mode operation utilized proton transfer reaction of positively charged water clusters with the analyte.

Experiments typically began with the addition of the reactants into the chamber. A known amount of liquid isoprene, MVK, or MACR was injected into a glass bulb, vaporised into the chamber, and then allowed to mix. Photolysis of nitrous acid (HONO) was used as the OH source. HONO was prepared by adding 1 wt % aqueous NaNO$_2$ drop wise into 10 wt % sulphuric acid and then introduced into the chamber using an air stream before the experiment started. Additional NO and NO$_2$ were added to the initial concentrations indicated in Table 2. Experiment time started when the black lights were turned on. No further additions were made to the chamber after the black lights were turned on. Total irradiation times for each experiment were approximately 8 hrs. A representative high-NO$_x$ isoprene experiment is shown in Fig. 1.

3 Determination of first-generation yields

Observed mixing ratios reflect both production and loss of each compound. To calculate total production yields, it is necessary to correct for the amount of product lost via photolysis and reaction with OH and O$_3$. This requires knowledge of the reaction rates with OH (k_{OH+X}) and O$_3$ (k_{OH+X}) (taken from the MCM), the O$_3$ concentration (which was measured), the photolysis rates (inferred from the measured glyoxal photolysis rate, see Sect. 3.1), as well as the OH concentration (inferred from the rate of change of observed VOCs, see Sect. 3.2).
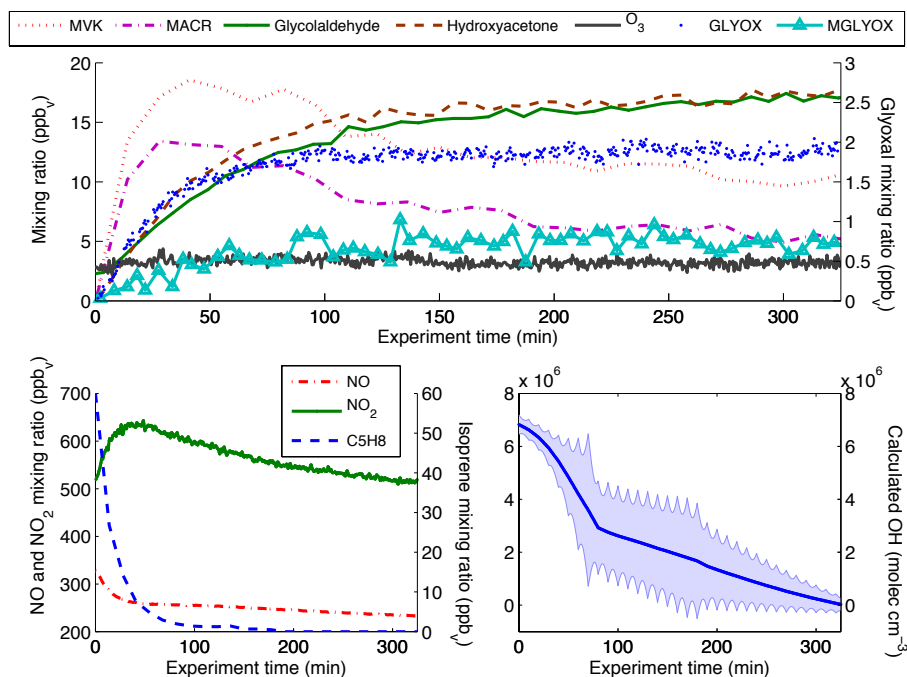
Fig. 1. Timeseries of measured compounds for Exp. 7. OH is the average of that calculated from ISP, MVK, and MACR. See Supplement for details about OH calculations.

3.1 Calculating photolysis rates

The glyoxal photolysis rate was measured during the 2008 experiments (Exp. Chan 1, Table S1, Chan et al., 2009) and again during the 2010 experiments (Exp. 1) to account for changes in blacklight intensity. Glyoxal photolysis in 2010 (0.14 h^{-1}) was 74% of the value in 2008 (0.19 h^{-1}), so the 2009 photolysis rate was interpolated between these values. The photolysis rates calculated from these experiments were used as a basis to estimate the photolysis rates of all other compounds. Photolysis rates in the MCM are given as a function of solar zenith angle (SZA), so the measured glyoxal photolysis rate was used to calculate an estimated SZA from the MCM; this was then used to calculate the photolysis rates for all other species.

3.2 Determining OH concentrations

OH number densities were estimated from the rate of loss of VOCs. Loss of VOC via reaction with O$_3$ and photolysis was taken into account by iteratively solving the loss equation for the precursor VOC, rearranged to solve for [OH],

$$[OH] = -\frac{1}{k_{OH+X}}\left(\frac{1}{[X]_{i-1}}\frac{\Delta[X]}{\Delta t} + k_{O_3+X}[O_3]_i + J_X\right) \quad (1)$$

where $[X]_{i-1}$ is the number density of the VOC X of measurement $i-1$, $\frac{\Delta[X]}{\Delta t}$ is the change in number density per unit time, k_{OH+X} and k_{O_3+X} are the rate constants for reaction with OH and O$_3$, respectively, and J_X is the photolysis rate of VOC X. Due to scatter in the precursor VOC

number densities, these data were fit to an exponential or double exponential before calculations. For the isoprene experiments, OH was calculated from isoprene until isoprene number density dropped below the limit of detection of the GC-FID (0.5 ppb, 1–2 h after experiment start), after which MVK and MACR data were used. OH was determined to be the mean of that calculated from MVK and MACR at each step. Due to the small change in VOCs at a 1 min timebase, OH was calculated on a 10 min timebase and then interpolated to a 1 min timebase for use in calculating first-generation yields. In general, OH was calculated to be 1×10^6–1×10^7 molec cm^{-3} at the start of the experiment and decreased to 1×10^4 molec cm^{-3} towards the end of the experiments. The uncertainty in OH was generally low (near 5%), at the beginning of the experiments but increased to as high as 250% as the primary VOC concentrations decreased. Figure S1 shows the calculated OH along with several measured time series for a typical.

3.3 Loss correction

Number densities of each product corrected to account for reaction with OH and O$_3$, [Y]^{corr}, were determined iteratively using the following recursive discrete time equation:

$$[Y]_i^{corr} = [Y]_{i-1}^{corr} + \Delta[Y]_i + [Y]_{i-1}\Delta t \left(k_{OH+Y}[OH] \right.$$
$$\left. + k_{O_3+Y}[O_3] + J_Y\right) \quad (2)$$

where [Y]$_i^{corr}$ is the corrected number density of the compound at measurement time i, [Y]$_{i-1}$ is the measured product

concentration of measurement $i-1$, Δt is time between measurements i and $i-1$, $\Delta[Y]_i$ is the observed net change in $[Y]$ that occurs over Δt, k_{OH+Y} and k_{O_3+Y} are the respective rate constants, and J_Y is the photolysis rate constant of the product Y. At any given time during the experiment, $[Y]^{corr}$ is equivalent to the total amount of Y which was produced up to that point, neglecting all loss processes. Figure S2 shows the loss corrected glyoxal concentrations for Exp. 3.

3.4 First-generation yields

The relationship between the loss corrected concentrations of reaction products and the amount of precursor VOC consumed via reaction is an indicator of first- versus higher-generation formation. VOCs react with OH, forming peroxy radicals, which then react largely with NO, giving alkoxy radicals and other species. First-generation reactions are those that stem from the initial OH attack and which do not involve another attack by OH, O$_3$, or NO$_3$ on one of the stable products. Therefore, a first generation product is the first stable product which results from one OH reacting with the precursor VOC. This first-generation product is formed at the same rate at which the precursor VOC is lost to reaction, therefore the relationship between these quantities is linear, as can be seen with the first generation formation of glycolaldehyde from 2-methyl-3-buten-2-ol (MBO) in Fig. S3. In contrast, a lag in the appearance of the product demonstrates that the reaction involves intermediates, as production does not depend on the reaction of the primary VOC but rather on that of a first- or later-generation product (Fig. S3). The slope of the line observed for the loss corrected product concentration versus reacted VOC corresponds to the first-generation yield (Fig. 2). This relationship can be expressed with a simple linear relationship:

$$[prod]_{corr} = a[VOC]_{reacted} + b \qquad (3)$$

where $[prod]_{corr}$ is the corrected product formed, $[VOC]_{reacted}$ is the amount of primary VOC reacted, and a is the first-generation yield.

first-generation yields were determined for each of the measured oxidation products in these experiments using the methods described above (Table 1). A representative isoprene oxidation experiment is shown in Fig. 1; the first-generation glyoxal yield calculated from this experiment is $2.32\,(\pm 0.01)\,\%$. The first-generation yields of MVK and MACR from isoprene presented here agree well with Tuazon and Atkinson (1990a). The first-generation glyoxal yield from isoprene calculated from our work is in the upper range (0.3–3 %) presented by Volkamer et al. (2006). Of the species studied here, the MCM includes only first-generation formation of MVK and MACR from isoprene, for which the yields are also shown in Table 1. Although first-generation formation of the two and three carbon species listed in Table 1 from isoprene is not included in the MCM or other com-
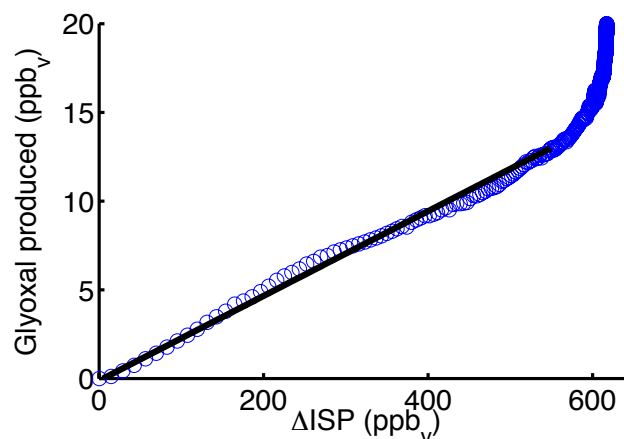
Fig. 2. Glyoxal production as a function of isoprene reacted in Exp. 2. Note the linear relationship between glyoxal and isoprene reacted in the first part of the experiment. The continued upward trend in glyoxal after isoprene is consumed corresponds to the formation of glyoxal as a higher generation oxidation product. The first-generation glyoxal yield for this experiment is 2.4 (± 0.013) %.

mon mechanisms, Dibble (2004a,b) has presented a possible reaction pathway in a theoretical study. The Dibble mechanism rationalizes first-generation formation of glyoxal together with hydroxyacetone and first-generation formation of methylglyoxal together with glycolaldehyde from isoprene via intramolecular hydrogen shift reactions of the radical intermediates in the presence of NO. The glyoxal, glycolaldehyde and hydroxyacetone observed in the work presented here agree with the Dibble mechanism, as does the work by Paulot et al. (2009a), who also observed first-generation production of glycolaldehyde and hydroxyacetone from reaction of isoprene and OH with similar yields. Due to the time resolution of the methylglyoxal data, we were unable to determine a first-generation methylglyoxal yield from isoprene. However, inclusion of a first-generation yield in the model resulted in good model-measurement agreement (see Sect. 4.3 and Fig. 3).

The first-generation yields of glycolaldehyde and methylglyoxal from MVK in this study agree within error to those found by Tuazon and Atkinson (1989). The same authors also determined a first-generation yield for hydroxyacetone from MACR (Tuazon and Atkinson, 1990b); our yield is on the high end of this range, but is in good agreement with the yield determined by Orlando et al. (1999). The first-generation yield of methylglyoxal from MACR in this work is lower but similar to that determined by Tuazon and Atkinson (1989), whereas the yield inferred by Paulot et al. (2009a) is substantially higher. Overall, the first-generation yields determined in this work agree with previously reported literature values.
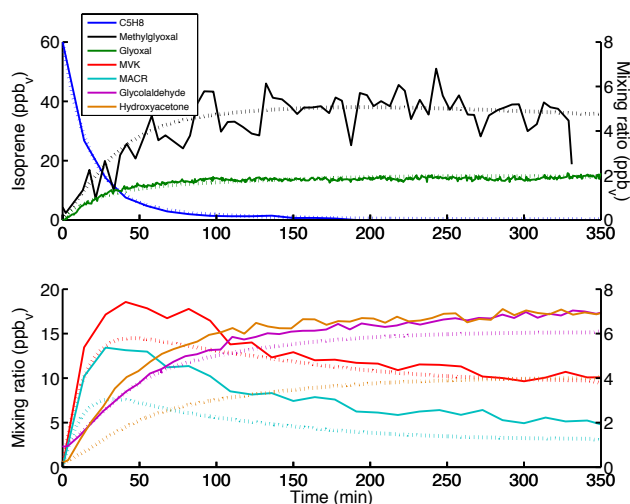
Fig. 3. Model and measurement comparison for high-NO$_x$ isoprene oxidation (Exp. 7) using the modified MCM model. The glycolaldehyde to glyoxal yield was set to 29 %, and first generation yields of glyoxal (2.6 %), methylglyoxal (2.7 %), hydroxyacetone (2.6 %), and glycolaldehyde (2.7 %) were included in this model run. Glyoxal production from C5 hydroxycarbonyls was attenuated to 1/6 of the MCM v. 3.2 values.

4 Comparison of first and higher generation yields with the MCM

4.1 MCM based model parameters

The MCM based photochemical box model described in detail by Huisman et al. (2011) was used to reproduce chamber results with minor modifications to the model parameters. O$_3$, NO$_2$, and air temperature were constrained to match measurements. However, for these chamber runs, the primary VOC and NO concentrations were not constrained to the measurements but predicted by the model after initialization with the observed initial values. This allowed for validation of the effectiveness of the model and OH calculations. Two features of the box model are the use of an SZA derived from measured photolysis rates (Sect. 3.1) and the use of chamber-derived OH (Sect. 3.2). Raw NO$_2$ data were corrected for detector saturation ([NO$_2$] > 1000 ppb$_v$) using a cubic spline fitting routine. In very dry, low aerosol conditions such as those in these experiments, glyoxal has been demonstrated to have negligible wall losses, and wall and aerosol losses are expected to be a minor to negligible sink of the other VOCs as well (Loza et al., 2010). Therefore, wall and aerosol losses are neglected in the model.

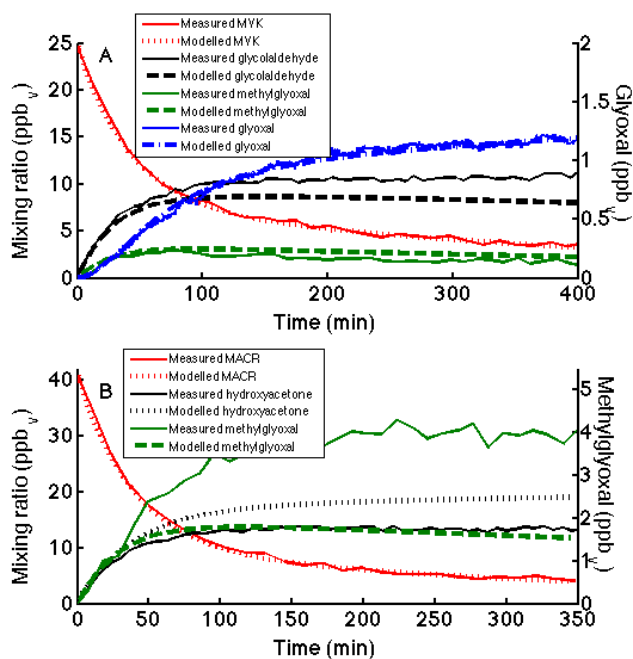### 4.2 Assessment of unmodified MCM

Model performance is assessed using a quality of fit parameter that takes into account the slope, correlation coefficient (R^2), and absolute residuals between measurement

and model (see Supplement Sect. 2 for details). The fit is evaluated for a short time, usually less than 1 h after experiment start, which reflects primarily first-generation production, and evaluated again for the remainder of the experiment, corresponding to a convolution of first and higher generation production. The MCM based model was able to reproduce chamber results for oxidation of MBO upon inclusion of the 29 % yield of glyoxal from glycolaldehyde found by Chan et al. (2009). For the high-NO$_x$ isoprene oxidation experiments, the model predicted MVK and MACR well. In contrast, the model underpredicted glyoxal (Fig. 5), methylglyoxal, hydroxyacetone, and glycolaldehyde in the primary production regime. This demonstrates that, as expected from Sect. 3, a first-generation yield is necessary to bring the model into agreement with measurements in the early part of the experiments. In contrast, the model overpredicts glyoxal in the later, higher generation production regime by approximately a factor of two.

For the MVK high-NO$_x$ oxidation experiments, predicted glyoxal (Fig. 4a) agrees very well with measurement, and modelled glycolaldehyde and methylglyoxal only slightly exceed the measurements. In the high-NO$_x$ MACR oxidation experiments, measured hydroxyacetone is approx. 75 % of modelled after first generation production, and modelled methylglyoxal is approximately double measured in the later part of the experiment (see Fig. 4b).

4.3 Inclusion of first-generation yields in MCM model

The first-generation yields determined in Sect. 3.2 and Table 1 that are not included in the current version of the MCM were added to the MCM-based model, i.e. first-generation production of glyoxal, glycolaldehyde, hydroxyacetone and methylglyoxal from isoprene and first-generation methylglyoxal production from MACR. As our results for first-generation formation of methylglyoxal from isoprene were inconclusive, we used the same value as that determined for glycolaldehyde following the work of Dibble (2004a,b) and Paulot et al. (2009a). Glyoxal and hydroxyacetone are formed through the same pathway, so the first-generation yield in the model was set to the average of those found in this study. Figure S4 shows the details of the modifications made to the MCM. The yields of hydroxyacetone, glycolaldehyde and glyoxal (see Table 1) are similar to but smaller (by 25–45 %) than those observed (or inferred for the case of glyoxal) by Paulot et al. (2009a) with exception of the first-generation yield of methylglyoxal from MACR, which is substantially lower in our work than the inferred value, but close to the yield determined by Tuazon and Atkinson (1990b). The unaltered MCM based model and a model with the first-generation yields were used to simulate chamber experiments of oxidation of isoprene, MVK, and MACR. Inclusion of the first-generation yields improved the model performance at early times in the isoprene and MACR studies (see Fig. 5 for a representative example), clearly supporting
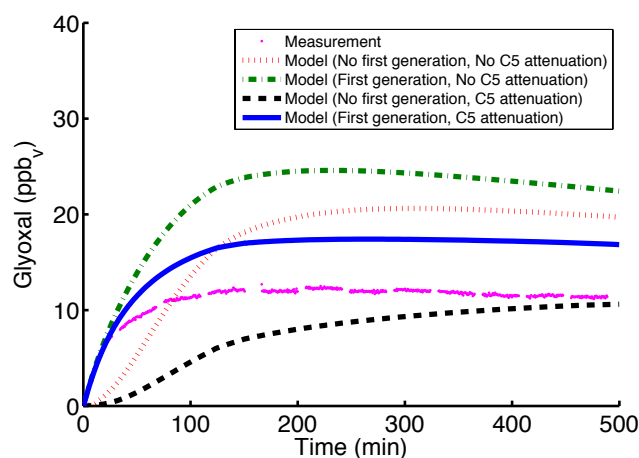
Fig. 5. Comparison of measured glyoxal concentration and MCM prediction for Exp. 2. Attenuation of glyoxal production from C5 hydroxycarbonyls to 1/6 of MCM v. 3.2 values brings the model into closer agreement with measurement during the latter part of the experiment. First-generation glyoxal yield is set to 2.6 %.

Fig. 4. **(A)** Modified MCM v. 3.2 Model and measurement comparison for high-NO$_x$ MVK oxidation (Exp. 8). The left axis corresponds to all compounds except glyoxal. The glycolaldehyde to glyoxal yield was set to 0.29 for this model run. **(B)** MCM v. 3.2 Model and measurement comparison for high-NO$_x$ MACR oxidation (Exp. 10). Note the discrepancy between measurement and model in both the hydroxyacetone and methylglyoxal once secondary production begins to dominate production.

the finding that these first-generation formation pathways should be incorporated into chemical mechanisms. For the best model performance, it was necessary to adjust the first-generation yields of glyoxal, methylglyoxal, glycolaldehyde, and hydroxyacetone to match those determined in each individual experiment. However, using the average of the calculated yields does improve the performance at early times for all experiments.

4.4 Attenuation of higher generation glyoxal production in the MCM

While the inclusion of first-generation production of glyoxal allowed the model to match early experimental results, the model still had a substantial overprediction of glyoxal at later times ($t > 1$ h) when the majority of isoprene had already been processed. This implies that glyoxal as a higher generation oxidation product of isoprene is significantly over expressed in the MCM for the conditions of our chamber experiments. An overexpression of secondary glyoxal production of an MCM model compared to measurements was also found but not reported in the study by Volkamer et al. (2006) (R. Volkamer, personal communication 2011). There are several channels that produce glyoxal (see Fig. 6); the

glyoxal yield from glycolaldehyde is known and glycolaldehyde was reproduced well in the later part of experiments, first-generation production of glyoxal from isoprene was determined experimentally, and the model is able to adequately reproduce glyoxal from both MVK and MACR oxidation experiments. The discrepancies in glyoxal production from isoprene oxidation are hence unlikely to result from any of these channels (Fig. 6). The majority of glyoxal not produced through these channels is formed through two C5 hydroxycarbonyl pathways (Fig. 6); therefore we adjusted the yield of glyoxal from these carbonyls in the MCM. Berndt and Böge (2007) observed a 17 % yield of glyoxal from the reaction of 4-hydroxy-2-butenal with OH, indicating that the C5 hydroxycarbonyls produce glyoxal, but possibly in lower quantities than predicted by the MCM. Therefore, the yields of glyoxal from the C5 hydroxycarbonyls were reduced in the modified MCM model.

Using the observed first-generation yield for glyoxal in the isoprene experiments, a model variant in which production of glyoxal from C5 hydroxycarbonyls was adjusted improved model performance markedly (Fig. 5). By reducing the higher generation production of glyoxal from C5 hydroxycarbonyls to 1/6 of the value in the MCM v. 3.2, most of the glyoxal production from isoprene oxidation can be modelled through first-generation formation from isoprene and the oxidation of glycolaldehyde. Glyoxal production from C5 hydroxycarbonyls is not necessarily wrong in the MCM; there are several other reasons why this attenuation might improve model performance. These include a missing C5 hydroxycarbonyl sink, such as C5 hydroxycarbonyl wall loss in the chambers, or incorrect reaction rates to form glyoxal. Attenuating the glyoxal production from these compounds is the easiest way to achieve attenuation in this study, and further
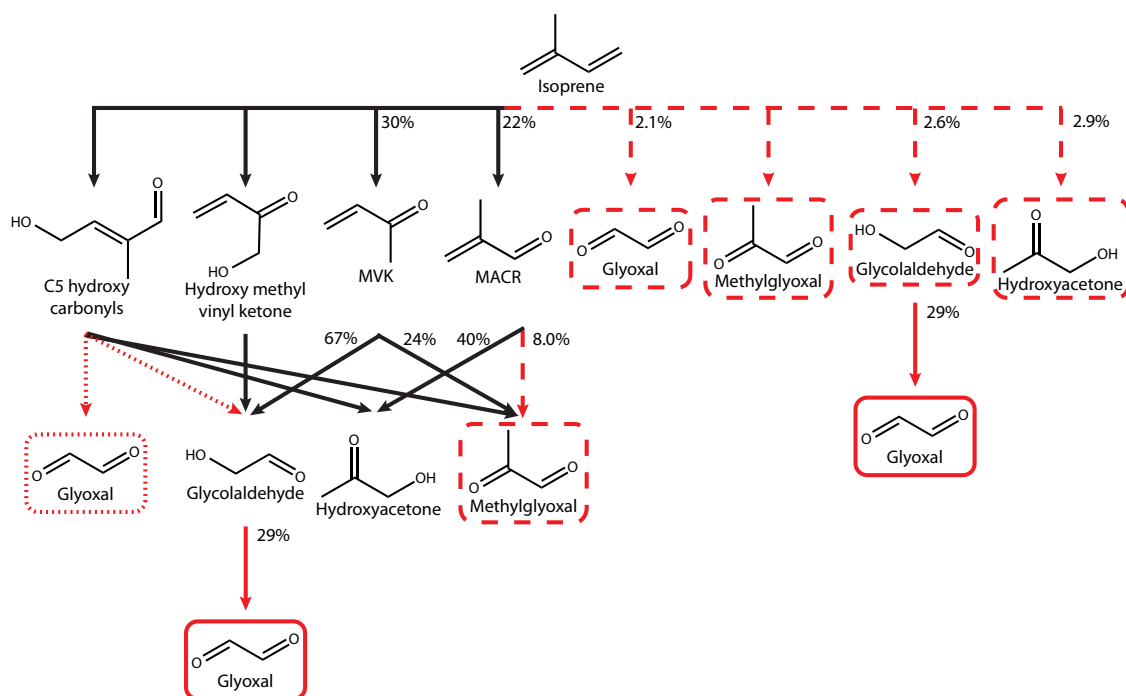
Fig. 6. Isoprene oxidation scheme. Dashed lines indicate first-generation formation pathways not included in the MCM. The dashed MACR to methylglyoxal line was not included in MCM v. 3.1, but is included in MCM v. 3.2 and was confirmed in this study. Dotted lines indicate the modifications to glyoxal production from C5 hydroxycarbonyls to 1/6 of the MCM v. 3.2 yield in our modelling studies. The solid red line indicates a yield verified by measurements with this study and the study by Chan et al. (2009). Yields given are those found in this study. The C5 hydroxycarbonyl shown here is one of multiple isomers in the MCM, which refers to them as HC4CCHO (shown here) and HC4ACHO.

experiments to study C5 hydroxycarbonyl formation and oxidation are necessary to fully understand glyoxal production from isoprene. Even with the complete removal of removing glyoxal production from C5 hydroxycarbonyls, modelled glyoxal is still slightly higher than measurements and the model modifications addressed above do not bring the measurement and model into perfect agreement, the model overpredicts glyoxal measurements by approx. 50 % at the end of experiments (Fig. 5). This could be due to the fact that OH is not measured, but is calculated from the isoprene, MVK, and MACR decay or may indicate that more studies must be done to understand this glyoxal production pathway. However, OH calculated from MVK and MACR is quite low and sensitivity analyses show that lowering it further has little impact, whereas raising it, which is the more likely error, would further increase modelled glyoxal.

4.5 Total product yields from the MCM

Once the model parameters were set to reproduce the measured species of interest, the altered MCM-based model was used to determine total yields of each of the products studied from isoprene, MVK, and MACR. To do this, the OH, O$_3$, NO$_2$, and air temperature inputs were extended at the final measured value ([O$_3$] = 320 ppb; OH = 8.2 ×

10^5 molec cm^{-1}) and the model was allowed to run using the modified MCM or unaltered MCM v. 3.2 until all products of interest were consumed. We also performed analogous model runs but with [O$_3$] = 0 ppb, to investigate the effect of the high ozone to OH ratio. The total amount of each compound produced was compared to the total consumption of the precursor VOC. The results of these model runs are shown in Table 3. The exclusion of ozone chemistry increases the glyoxal yields, as glyoxal is primarily formed via OH-driven chemistry and this effect is stronger for the original MCM v. 3.2 than for the modified version. It should be noted that the measured glyoxal yields at the end of the experiment are only about 68 % and 64 % of those modelled with the modified and original MCM v. 3.2, respectively, which correspond to results in column 2 and 3 in Table 3. The fact that the original MCM v. 3.2 overpredicts glyoxal more at the end of the experiment but has a lower total yield results from the fact that it has higher second-generation production (from the C5 hydroxycarbonyls) than the modified MCM, whereas the latter has increased third- (and higher) generation production via glycolaldehyde compared to MCM v. 3.2, due to the increased yield of glyoxal from glycolaldehyde from 20 % to 29 %.

Table 3. Total molar yields from isoprene oxidation calculated with the modified MCM and original MCM v. 3.2 for high NO$_x$ conditions. Total yields are calculated by allowing the model to run until species of interest have reacted away. Columns 2 and 3 are model simulations in which the conditions were held constant at the end of the experiment to determine total yields ([O$_3$] = 320 ppb; OH = 8.2×10^5 molec cm^{-1}). Columns 4 and 5 are for identical runs, except that [O$_3$] was set to 0 ppb. The observed glyoxal at the end of the experiments was only about 2/3 of the modelled output from columns 2 and 3.

Compound	Total Yield: mod. MCM [O$_3$]=320 ppb	Total Yield: MCM v. 3.2 [O$_3$]=320 ppb	Total Yield: mod. MCM [O$_3$]=0 ppb	Total Yield: MCM v. 3.2 [O$_3$]=0 ppb
MVK	40.7 %	40.7 %	41.6 %	41.6 %
MACR	26.8 %	26.8 %	26.6 %	26.6 %
Glycolaldehyde	24.8 %	24.3 %	40.9 %	41.6 %
Hydroxyacetone	23.0 %	22.1 %	22.5 %	22.5 %
Glyoxal	9.6 %	8.0 %	10.3 %	11.0 %
Methylglyoxal	35.0 %	35.2 %	27.1 %	26.4 %

5 Conclusions

We present yields of first-generation oxidation products of isoprene, MVK, and MACR, several of which are not included in current chemical mechanisms, such as the MCM. Inclusion of first-generation production of glyoxal, glycolaldehyde and hydroxyacetone from isoprene and methylglyoxal from MACR greatly improved performance of a MCM based model during the first few hours of oxidation. However, inclusion of the first-generation glyoxal yield degraded the already poor performance of the MCM based model during the higher generation production phase of the isoprene experiments. It was necessary to scale down higher generation glyoxal production from isoprene in order to prevent substantial overprediction in relation to chamber experiments. Reducing the glyoxal production from C5 carbonyls greatly improved model performance, indicating that this pathway could be overexpressed in the MCM. However, further work is needed to determine whether the cause of the over prediction is indeed from the fate of C5 hydroxycarbonyls, which could not be ascertained in this work. The C5 hydroxycarbonyls were detected by the CIMS and the signals were quite low. However, no calibration is available and as no experiments with the C5 hydroxycarbonyls themselves were conducted, no quantitative analysis was possible, demonstrating that further work on these compounds is necessary; in addition, the high glyoxal yield from glycolaldehyde of 29 % in this study should be verified, as an overestimate of this yield could explain part of the discrepancy at later experiment times. In addition, secondary oxidation processes are typically slower and occur at lower OH concentrations, which results in increased uncertainties in the secondary chemistry. Measurements of OH, particularly during the part of experiments dominated by secondary chemistry, would help to better constrain mechanisms.

The results presented here furthermore suggest that glyoxal production from reaction of OH with isoprene under high NO$_x$ conditions can be approximated, e.g. for models requiring simplified mechanisms, by inclusion of only a first-generation production term together with secondary production via glycolaldehyde, which simplifies the MCM isoprene mechanism for glyoxal. Similarly, we propose that methylglyoxal production can be approximated by a first-generation production term from isoprene, and secondary production via MVK, MACR and hydroxyacetone (Fig. 6).

Atmospheric implications

The first-generation yields of glyoxal, methylglyoxal, hydroxyacetone, and glycolaldehyde correspond to less than 5 % of the total isoprene yield and thus only have a small effect on the overall fate of isoprene. However, due to the abundance of isoprene, these findings together with the reduced higher generation production of glyoxal from C5 hydroxycarbonyls are important for models that investigate the production of the small oxidized organic molecules, especially within the context of SOA formation and cloud processing. Fu et al. (2008, 2009) used the GEOS-Chem global model updated with oxidation chemistry from the MCM to determine global aerosol yields from glyoxal and methylglyoxal. The global annual mean yields of glyoxal and methylglyoxal from OH reaction with isoprene as calculated by GEOS-Chem were 8 % and 29 %, respectively. The global glyoxal molar yield from isoprene in the study by Stavrakou et al. (2009) was found to be only slightly (16 %) higher than in the GEOS-Chem model. These glyoxal yields are close to the yields reported in this work (Table 3). However, these studies are missing the first-generation production term. Subtraction of 5/6 of the GEOS-Chem glyoxal yield via C5 hydroxycarbonyls (3.15 %) from the total glyoxal yield predicted by GEOS-Chem results in a higher-generation glyoxal yield from isoprene of 4.85 %. With the addition of the first-generation glyoxal yield from isoprene in this study (2.1 %),

an overall glyoxal yield of 6.95 % from OH reaction with isoprene is predicted, which is lower than that found in our altered and unaltered MCM model runs. However, it should be kept in mind that the modelled glyoxal was about 50 % higher than observed; scaling our total yield of 9.6 % by this amount gives 6.4 %, very close to the modified yields of Fu et al. (2008) and Fu et al. (2009), corrected for direct production and attenuated higher generation production from C5-hydroxycarbonyls. The yields observed in this study suggest that global models discussed above may be overestimating glyoxal production from isoprene by about 15 %, not a large amount. However, comparison of current global models with satellite glyoxal observations actually shows an underestimation of glyoxal over biogenically active regions (Stavrakou et al., 2009). If such discrepancies are true (and not due to satellite observation error or model isoprene emission error), then attenuation of the glyoxal yield from isoprene would aggravate the discrepancy. This, in turn, would mean that the missing biogenic source of glyoxal suggested by Stavrakou et al. (2009) is even larger than previously thought.

In addition, this work demonstrates that even for a molecule that has been as extensively studied as isoprene, its oxidation mechanism remains uncertain. Although the intramolecular rearrangements as proposed by Dibble (2004a,b) are not likely to correspond to the major channels, they can have a substantial impact on species that are produced in lower concentrations. The results presented here support the existence of such intramolecular rearrangements as do the results of (Paulot et al., 2009a) and Volkamer et al. (2006), which has implications for other cases for which similar rearrangements have been proposed, including OH recycling (Peeters et al., 2009).

Supplementary material related to this article is available online at: http://www.atmos-chem-phys.net/11/10779/2011/ acp-11-10779-2011-supplement.pdf.

References

Altieri, K., Seitzinger, S., Carlton, A., Turpin, B., Klein, G., and Marshall, A.: Oligomers formed through in-cloud methylglyoxal reactions: Chemical composition, properties, and mechanisms investigated by ultra-high resolution FT-ICR mass spectrometry, Atmos. Environ., 42, 1476–1490, doi:10.1016/j.atmosenv.2007.11.015, 2008.

Archibald, A. T., Cooke, M. C., Utembe, S. R., Shallcross, D. E., Derwent, R. G., and Jenkin, M. E.: Impacts of mechanistic changes on HO$_x$ formation and recycling in the oxidation of isoprene, Atmos. Chem. Phys., 10, 8097–8118, doi:10.5194/acp-10-8097-2010, 2010a.

Archibald, A. T., Jenkin, M. E., and Shallcross, D. E.: An isoprene mechanism intercomparison, Atmos. Environ., 44, 5356–5364, doi:10.1016/j.atmosenv.2009.09.016, 2010b.

Berndt, T. and Böge, O.: Atmospheric Reaction of OH Radicals with 1,3-Butadiene and 4-Hydroxy-2-butenal, J. Phys. Chem. A, 111, 12099–12105, doi:10.1021/jp075349o, 2007.

Carlton, A., Turpin, B., Altieri, K., Seitzinger, S., Reff, A., Lim, H., and Ervens, B.: Atmospheric oxalic acid and SOA production from glyoxal: Results of aqueous photooxidation experiments, Atmos. Environ., 41, 7588–7602, doi:10.1016/j.atmosenv.2007.05.035, 2007.

Carlton, A. G., Wiedinmyer, C., and Kroll, J. H.: A review of Secondary Organic Aerosol (SOA) formation from isoprene, Atmos. Chem. Phys., 9, 4987–5005, doi:10.5194/acp-9-4987-2009, 2009b.

Chan, A. W. H., Galloway, M. M., Kwan, A. J., Chhabra, P. S., Keutsch, F. N., Wennberg, P. O., Flagan, R. C., and Seinfeld, J. H.: Photooxidation of 2-methyl-3-buten-2-ol (MBO) as a potential source of secondary organic aerosol, Environ. Sci. Technol., 43, 4647–4652, doi:10.1021/es802560w, 2009.

Cocker, D. R., Flagan, R. C., and Seinfeld, J. H.: State-of-the-art chamber facility for studying atmospheric aerosol chemistry, Environ. Sci. Technol., 35, 2594–2601, doi:10.1021/Es0019169, 2001.

Crounse, J., McKinney, K., Kwan, A., and Wennberg, P.: Measurement of gas-phase hydroperoxides by chemical ionization mass spectrometry, Anal. Chem., 78, 6726–6732, doi:10.1021/ac0604235, 2006.

Dibble, T. S.: Intramolecular hydrogen bonding and double H-atom transfer in peroxy and alkoxy radicals from isoprene, J. Phys. Chem. A, 108, 2199–2207, doi:10.1021/jp0306702, 2004a.

Dibble, T. S.: Prompt chemistry of alkenoxy radical products of the double H-atom transfer of alkoxyradicals from isoprene, J. Phys. Chem. A, 108, 2208–2215, doi:10.1021/jp0312161, 2004b.

Ervens, B., Carlton, A. G., Turpin, B. J., Altieri, K. E., Kreidenweis, S. M., and Feingold, G.: Secondary organic aerosol yields from cloud-processing of isoprene oxidation products, Geophys. Res. Lett., 35, L02816, doi:10.1029/2007gl031828, 2008.

Fan, J. and Zhang, R.: Atmospheric Oxidation Mechanism of Isoprene, Environ. Chem., 1, 140–149, doi:10.1071/EN04045, 2004.

Fu, T.-M., Jacob, D. J., Wittrock, F., Burrows, J., Vrekoussis, M., and Henze, D.: Global budgets of atmospheric glyoxal and methylglyoxal, and implications for formation of secondary organic aerosols, J. Geophys. Res., 113, D15303, doi:10.1029/2007JD009505, 2008.

Fu, T.-M., Jacob, D. J., and Heald, C. L.: Aqueous-phase re-

active uptake of dicarbonyls as a source of organic aerosol over eastern North America, Atmos. Environ., 43, 1814–1822, doi:10.1016/j.atmosenv.2008.12.029, 2009.

Galloway, M. M., Chhabra, P. S., Chan, A. W. H., Surratt, J. D., Flagan, R. C., Seinfeld, J. H., and Keutsch, F. N.: Glyoxal uptake on ammonium sulphate seed aerosol: reaction products and reversibility of uptake under dark and irradiated conditions, Atmos. Chem. Phys., 9, 3331–3345, doi:10.5194/acp-9-3331-2009, 2009.

Galloway, M. M., Loza, C. L., Chhabra, P. S., Chan, A. W. H., Yee, L. D., Seinfeld, J. H., and Keutsch, F. N.: Analysis of photochemical and dark glyoxal uptake: Implications for SOA formation, Geophys. Res. Lett., 38, L17811, doi:10.1029/2011GL048514, 2011.

Gu, C. L., Rynard, C. M., Hendry, D. G., and Mill, T.: Hydroxide radical oxidation of isoprene, Environ. Sci. Technol., 19, 151–155, doi:10.1021/es00132a007, 1985.

Guenther, A., Hewitt, C., Erickson, D., Fall, R., Geron, C., Graedel, T., Harley, P., Klinger, L., Lerdau, M., Mckay, W., Pierce, T., Scholes, B., Steinbrecher, R., Tallamaraju, R., Taylor, J., and Zimmerman, P.: A global model of natural volatile organic-compound emissions, J. Geophys. Res.-Atmos., 100, 8873–8392, doi:10.1029/94JD02950, 1995.

Henry, S. B., Kammrath, A., and Keutsch, F. N.: Quantification of gas-phase glyoxal and methylglyoxal via the Laser-Induced Phosphorescence of (methyl)GLyOxal Spectrometry (LIPGLOS) method, Atmos. Meas. Tech. Discuss., 4, 6159–6183, doi:10.5194/amtd-4-6159-2011, 2011.

Huisman, A. J., Hottle, J. R., Coens, K. L., DiGangi, J. P., Galloway, M. M., Kammrath, A., and Keutsch, F. N.: Laser-induced phosphorescence for the in situ detection of glyoxal at part per trillion mixing ratios, Anal. Chem., 80, 5884–5891, doi:10.1021/ac800407b, 2008.

Huisman, A. J., Hottle, J. R., Galloway, M. M., DiGangi, J. P., Coens, K. L., Choi, W. S., Faloona, I. C., Gilman, J. B., Kuster, W. C., de Gouw, J., Bouvier-Brown, N. C., Goldstein, A. H., LaFranchi, B. W., Cohen, R. C., Wolfe, G. M., Thornton, J. A., Docherty, K. S., Farmer, Delphine, K., Cubison, Jimenez, J. L., M. J., Mao, J., Brune, W. H., and Keutsch, F. N.: Photochemical modeling of glyoxal at a rural site: observations and analysis from BEARPEX 2007, Atmos. Chem. Phys., 11, 8883–8897, doi:10.5194/acp-11-8883-2011, 2011.

Ip, H. S. S., Huang, X. H. H., and Yu, J. Z.: Effective Henry's law constants of glyoxal, glyoxylic acid, and glycolic acid, Geophys. Res. Lett., 36, L01802, doi:10.1029/2008GL036212, 2009.

Jenkin, M. E., Saunders, S. M., and Pilling, M. J.: The tropospheric degradation of volatile organic compounds: a protocol for mechanism development, Atmos. Environ., 31, 81–104, doi:10.1016/s1352-2310(96)00105-7, 1997.

Karl, T., Guenther, A., Turnipseed, A., Tyndall, G., Artaxo, P., and Martin, S.: Rapid formation of isoprene photo-oxidation products observed in Amazonia, Atmos. Chem. Phys., 9, 7753–7767, doi:10.5194/acp-9-7753-2009, 2009.

Keywood, M. D., Varutbangkul, V., Bahreini, R., Flagan, R. C., and Seinfeld, J. H.: Secondary organic aerosol formation from the ozonolysis of cycloalkenes and related compounds, Environ. Sci. Technol., 38, 4157–4164, doi:10.1021/Es035363o, 2004.

Kwok, E. S. C., Atkinson, R., and Arey, J.: Observation of Hydroxycarbonyls from the OH Radical-Initiated Reac-

tion of Isoprene, Environ. Sci. Technol., 29, 2467–2469, doi:10.1021/es00009a046, 1995.

Loza, C. L., Chan, A. W. H., Galloway, M. M., Keutsch, F. N., Flagan, R. C., and Seinfeld, J. H.: Characterization of vapor wall loss in laboratory chambers, Environ. Sci. Technol., 44, 5074–5078, doi:10.1021/es100727v, 2010.

Madronich, S. and Calvert, J. G.: The NCAR Master Mechanism of the gas phase chemistry-Version 2.0, Rep. NCAR/TN-333+STR, National Center for Atmospheric Research, 1989.

Miyoshi, A., Hatakeyama, S., and Washida, N.: OH radical-initiated photooxidation of isoprene: An estimate of global CO production, J. Geophys.Res.-Atmos., 99, 18779–18787, doi:10.1029/94JD01334, 1994.

Nozière, B., Dziedzic, P., and Cordova, A.: Products and kinetics of the liquid-phase reaction of glyoxal catalyzed by ammonium ions (NH$_4^+$), J. Phys. Chem. A, 113, 231–237, doi:10.1021/jp8078293, 2009.

Orlando, J. J., Tyndall, G. S., and Paulson, S. E.: Mechanism of the OH-initiated oxidation of methacrolein, Geophys. Res. Lett., 26, 2191–2194, doi:10.1029/1999gl900453, 1999.

Paulot, F., Crounse, J. D., Kjaergaard, H. G., Kroll, J. H., Seinfeld, J. H., and Wennberg, P. O.: Isoprene photooxidation: new insights into the production of acids and organic nitrates, Atmos. Chem. Phys., 9, 1479–1501, doi:10.5194/acp-9-1479-2009, 2009a.

Paulot, F., Crounse, J. D., Kjaergaard, H. G., Kurten, A., St. Clair, J. M., Seinfeld, J. H., and Wennberg, P. O.: Unexpected epoxide formation in the gas-phase photooxidation of isoprene, Science, 325, 730–733, doi:10.1126/science.1172910, 2009b.

Paulson, S. E., Flagan, R. C., and Seinfeld, J. H.: Atmospheric photooxidation of isoprene part I: The hydroxyl radical and ground state atomic oxygen reactions, Int. J. Chem. Kin., 24, 79–101, doi:10.1002/kin.550240109, 1992.

Peeters, J., Nguyen, T. L., and Vereecken, L.: HO$_x$ radical regeneration in the oxidation of isoprene, Phys. Chem. Chem. Phys., 11, 5935–5939, doi:10.1039/B908511d, 2009.

Perri, M. J., Seitzinger, S., and Turpin, B. J.: Secondary organic aerosol production from aqueous photooxidation of glycolaldehyde: Laboratory experiments, Atmos. Environ., 43, 1487–1497, doi:10.1016/j.atmosenv.2008.11.037, 2009.

Sareen, N., Schwier, A. N., Shapiro, E. L., Mitroo, D., and McNeill, V. F.: Secondary organic material formed by methylglyoxal in aqueous aerosol mimics, Atmos. Chem. Phys., 10, 997–1016, doi:10.5194/acp-10-997-2010, 2010.

Saunders, S. M., Jenkin, M. E., Derwent, R. G., and Pilling, M. J.: Protocol for the development of the Master Chemical Mechanism, MCM v3 (Part A): tropospheric degradation of non-aromatic volatile organic compounds, Atmos. Chem. Phys., 3, 161–180, doi:10.5194/acp-3-161-2003, 2003.

Shapiro, E. L., Szprengiel, J., Sareen, N., Jen, C. N., Giordano, M. R., and McNeill, V. F.: Light-absorbing secondary organic material formed by glyoxal in aqueous aerosol mimics, Atmos. Chem. Phys., 9, 2289–2300, doi:10.5194/acp-9-2289-2009, 2009.

Sprengnether, M., Demerjian, K. L., Donahue, N. M., and Anderson, J. G.: Product analysis of the OH oxidation of isoprene and 1,3-butadiene in the presence of NO, J. Geophys. Res., 107, 4268, doi:10.1029/2001jd000716, 2002.

St. Clair, J. M., McCabe, D. C., Crounse, J. D., Steiner, U., and Wennberg, P. O.: Chemical ionization tandem mass spectrom-

eter for the in situ measurement of methyl hydrogen peroxide, Rev. Sci. Instrum., 81, 094102–094106, doi:10.1063/1.3480552, 2010.

Stavrakou, T., Müller, J.-F., De Smedt, I., Van Roozendael, M., Kanakidou, M., Vrekoussis, M., Wittrock, F., Richter, A., and Burrows, J. P.: The continental source of glyoxal estimated by the synergistic use of spaceborne measurements and inverse modelling, Atmos. Chem. Phys., 9, 8431–8446, doi:10.5194/acp-9-8431-2009, 2009.

Tan, Y., Perri, M. J., Seitzinger, S. P., and Turpin, B. J.: Effects of precursor concentration and acidic sulfate in aqueous glyoxal-OH radical oxidation and implications for secondary organic aerosol, Environ. Sci. Technol. 43, 8105–8112, doi:10.1021/es901742f, 2009.

Taraborrelli, D., Lawrence, M. G., Butler, T. M., Sander, R., and Lelieveld, J.: Mainz Isoprene Mechanism 2 (MIM2): an isoprene oxidation mechanism for regional and global atmospheric modelling, Atmos. Chem. Phys., 9, 2751–2777, doi:10.5194/acp-9-2751-2009, 2009.

Tuazon, E. C. and Atkinson, R.: A product study of the gas-phase reaction of methyl vinyl ketone with the OH radical in the presence of NOₓ, Int. J. Chem. Kinet., 21, 1141–1152, doi:10.1002/kin.550211207, 1989.

Tuazon, E. C. and Atkinson, R.: A product study of the gas-phase reaction of isoprene with the OH radical in the presence of NOₓ, Int. J. Chem. Kin., 22, 1221–1236, doi:10.1002/kin.550221202, 1990a.

Tuazon, E. C. and Atkinson, R.: A product study of the gas-phase reaction of methacrolein with the OH radical in the presence of NOₓ, Int. J. Chem. Kin., 22, 591–602, doi:10.1002/kin.550220604, 1990b.

Volkamer, R., Barnes, I., Platt, U., Molina, L. T., and Molina, M. J.: Remote sensing of glyoxal by differential optical absorption spectroscopy (DOAS): Advancements in simulation chamber and field experiments, in: Environmental Simulation Chambers: Application to Atmospheric Chemical Processes, edited by: Barnes, I. and Rudinski, J., 62, Springer, Dordrecht, Netherlands, 2006.

Volkamer, R., Ziemann, P. J., and Molina, M. J.: Secondary organic aerosol formation from acetylene (C₂H₂): seed effect on SOA yields due to organic photochemistry in the aerosol aqueous phase, Atmos. Chem. Phys., 9, 1907–1928, doi:10.5194/acp-9-1907-2009, 2009.

Zhao, J., Zhang, R., Fortner, E. C., and North, S. W.: Quantification of Hydroxycarbonyls from OHIsoprene Reactions, J. Am. Chem. Soc., 126, 2686–2687, doi:10.1021/ja0386391, 2004.